

FULLY POLARIMETRIC L-BAND BRIGHTNESS TEMPERATURE SIGNATURES OF AZIMUTHAL PERMITTIVITY PATTERNS – MEASUREMENTS AND MODEL SIMULATIONS

Sten Schmidl Søbjerg¹, Moritz Link², Thomas Jagdhuber², Carsten Montzka³,
Francois Jonard^{3,4}, Stephan Dill², Markus Peichl², Thomas Meyer³

¹Technical University of Denmark, National Space Institute (DTU Space), Lyngby, Denmark
phone/fax: +45 4525 3767/+45 4593 1634, email: sss@space.dtu.dk

²German Aerospace Center, Microwaves and Radar Institute, Münchner Strasse 20, 82234 Wessling, Germany,

³Forschungszentrum Jülich, Institute of Bio- and Geosciences: Agrosphere (IBG-3), Jülich, Germany.

⁴Université catholique de Louvain, Earth and Life Institute, Louvain-la-Neuve, Belgium.

ABSTRACT

L-Band microwave radiometry over land mainly focuses on observations of horizontally (H) and vertically (V) polarized brightness temperatures. However, it has been demonstrated that measurements of the full Stokes vector [1] are sensitive to additional environmental properties, e.g. azimuthal plant row orientation. Furthermore, model simulations show that also a smooth surface with a periodic permittivity pattern can cause azimuthal dependencies of the Stokes parameters. The objective of this paper is to present fully polarimetric L-band measurement results from observations of a striped wood and styrodur target, when rotated 360° in small steps. Measurement results of a striped soil and open water target are also reported. Finally, measurements are compared to model simulations, with very good agreement within the validity range of the model (stripe thickness $< \lambda/2$).

Index Terms— Radiometry, Microwave, Polarimetry, L-band, Experiment

1. INTRODUCTION

The L-band passive microwave missions NASA/SMAP and ESA/SMOS [2] both aim at soil moisture estimation within the upper soil layers down to an accuracy of $\pm 0.04 \text{ cm}^3/\text{cm}^3$. L-band at 1.413 GHz ($\lambda \approx 21 \text{ cm}$) is the preferred frequency due to the presence of a protected bandwidth along with the low atmospheric influence and a fair vegetation penetration capability. Soil moisture inversion algorithms of both missions mainly focus on measurements of H- and/or V-polarized brightness temperatures, although they have the capability to acquire the full Stokes vector [1], shown in (1).

$$\overline{T}_B = \begin{pmatrix} I \\ Q \\ U \\ V \end{pmatrix} = \begin{pmatrix} T_V + T_H \\ T_V - T_H \\ T_{45^\circ} - T_{-45^\circ} \\ T_l - T_r \end{pmatrix} = \frac{\lambda^2}{k \cdot z} \begin{pmatrix} \langle E_V^2 \rangle + \langle E_H^2 \rangle \\ \langle E_V^2 \rangle - \langle E_H^2 \rangle \\ 2 \text{Re} \langle E_V E_H^* \rangle \\ 2 \text{Im} \langle E_V E_H^* \rangle \end{pmatrix} \quad (1)$$

Experiments show that observations of the full Stokes vector (besides the H- and V-polarized brightness temperatures) are sensitive to additional environmental properties like plant row alignment [3,4], periodic surface structures [5] etc. Moreover, model simulations in [6] indicate that also a smooth surface with a periodic permittivity pattern can cause azimuthal dependencies of all four Stokes parameters. However, measurements have only been conducted for validation of the model at higher frequencies (90 GHz), and hence this controlled field experiment is carried out in order to study azimuthal signatures at L-band.

Airborne campaign data sets, acquired for calibration and validation of SMOS in 2010 [7] indicate some polarimetric signals to be present, and the overall aim of this paper is to confirm the expected trends and magnitudes of the permittivity-induced azimuthal signal.

2. MODEL

An emission model for a smooth infinite half-space with alternating striped layers of widths d_1, d_2 and permittivities ϵ_1, ϵ_2 was developed in [6]. The model assumes that the layer widths are significantly smaller than the wavelength ($d_1, d_2 \ll \lambda$) such that the half-space acts as form-birefringent uniaxial crystal, i.e. the electromagnetic field is uniform in both permittivity layers and the directional permittivity of the overall medium can be expressed through a dyadic tensor [8]. The form birefringence leads to non-zero contributions in the Third and Fourth Stokes parameters and an azimuthal dependency of all Stokes parameters [6]. A full model description with mathematical formulations is found in [6] (in German).

We apply the model to simulate the L-band emissivity for layer widths in the range of 2-40 cm. The validity criterion ($d_1, d_2 \ll \lambda$) is hereby deliberately approached and violated to investigate the validity boundaries of the model for large layer thicknesses.

3. TEST SITE

The experiment is conducted at the TERENO (Terrestrial Environmental Observations) test site in Selhausen, Germany. The site features a setup for ground-based remote sensing, which is developed by the Forschungszentrum Jülich [9]. The site is seen in Figure 1.



Figure 1: The TERENO test site in Selhausen, Germany.

The arc is designed to carry the instrumentation, and the direction of observation is north in order to avoid possible reflected sun radiation. Furthermore the site is located in a rural area known to be free from Radio Frequency Interference (RFI) at L-band.

4. TARGET CONSTRUCTION

The measurement target is designed to be circular with a clear striped structure. The stripes are composed of wood and styrodur (permittivity difference, $\Delta\epsilon' \approx 2.5$) elements, each with a thickness of 2 cm. The stripes are arranged on top of a rotating platform, and an absorber is placed between the bottom of the platform and the elements in order to yield a neutral and fully symmetric background. A sketch of the setup is shown in Figure 2.

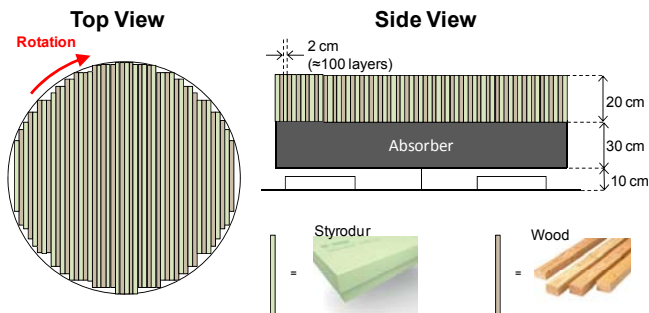


Figure 2: The rotating target. The absorber layer and the wood/styrodur assembly are placed on a platform, which can be rotated in steps down to 2.5° .

The rotating platform can be locked in positions, separated 2.5° , i.e. a total of 72 azimuthal positions can be sampled. Finally the whole structure is shielded by a wire grid with a mesh-size < 1 cm in order to avoid false

azimuthal signals from possible features on the rotating platform itself. Also the surrounding soil is covered by a wire grid to ensure a stable background (perfect reflector). The complete target can be seen in Figure 3.



Figure 3: The target assembly. A metal fence surrounds the target and covers the nearby soil to provide a stable background for the measurements.

The target elements can be rearranged for measurement series with different wood/styrodur layering width. Swapping every second set of wood/styrodur elements, the result will be two wood elements followed by two styrodur elements, and hence a striped structure with a layer thickness of 4 cm will result. In the same manner, layers of 8 cm, 16 cm, and 32 cm can be achieved. Finally the wood/styrodur elements can be replaced through layers of soil and open water or wet soil and dry soil. The purpose is to simulate a natural target with stripes from irrigation, and the setup is shown in Figure 4.



Figure 4: Target setup for measurements on stripes of dry soil and open water.

5. INSTRUMENTATION

Radiometric measurements are acquired using the fully polarimetric EMIRAD radiometer [10].

5.1. The EMIRAD radiometer

The EMIRAD radiometer is fully polarimetric, and hence it yields parallel measurements of the full Stokes vector. The radiometer is a correlation type polarimetric radiometer, and the digital back-end also features real-time RFI-detection through estimation of kurtosis. The radiometer uses a Potter horn antenna with -3 dB @ $\pm 15.3^\circ$ and -20 dB @ $\pm 38.5^\circ$ relative to the maximum gain at bore sight. The antenna is connected to the radiometer front through an Ortho Mode Transducer (OMT) and low-loss cables. A photograph of the EMIRAD radiometer mounted at the test site is seen in Figure 5.



Figure 5: The EMIRAD radiometer, including the Potter horn antenna and the Ortho Mode Transducer (OMT).

5.2. Radiometer calibration

The EMIRAD radiometer features a three-point internal calibration, followed by two additional calibration steps, compensating for external losses, cross coupling, and phase imbalances.

Internal calibration is based upon a hot load, and an Active Cold Load (ACL) in each channel. Furthermore, the internal calibration features a common active noise source, which provides a third calibration point and ensures phase coherence between the two channels in order to avoid mixing of the 3rd and 4th Stokes parameters. Observations of the internal calibration points are performed for each data point during the experiment.

External calibration compensates for losses in cables, and antenna/OMT. Cable losses are calibrated once per day, using a Liquid Nitrogen (LN2) cooled target, which is connected to the cables at the far end. The cables losses are stable within ± 0.01 dB throughout the entire experiment. Phase differences, φ , for the cables are measured prior to and after the campaign using a Keysight Fieldfox N9918A Vector Network Analyzer (VNA), and they remain stable within 1° . Phase differences are corrected using (2).

$$\overline{T}_B' = \begin{pmatrix} I' \\ Q' \\ U' \\ V' \end{pmatrix} = \begin{pmatrix} 1 & 0 & 0 & 0 \\ 0 & 1 & 0 & 0 \\ 0 & 0 & \cos(\varphi) & -\sin(\varphi) \\ 0 & 0 & \sin(\varphi) & \cos(\varphi) \end{pmatrix} \begin{pmatrix} I \\ Q \\ U \\ V \end{pmatrix} \quad (2)$$

The phase difference in the OMT is estimated using the same VNA, and likewise the channel coupling, ρ , is measured. Equations (2) and (3) apply the corrections.

$$\overline{T}_B' = \begin{pmatrix} I' \\ Q' \\ U' \\ V' \end{pmatrix} = \begin{pmatrix} 1 & 0 & 0 & 0 \\ 0 & 1-2\rho & 0 & -2\sqrt{\rho-\rho^2} \\ 0 & 0 & 1 & 0 \\ 0 & 2\sqrt{\rho-\rho^2} & 0 & 1-2\rho \end{pmatrix} \begin{pmatrix} I \\ Q \\ U \\ V \end{pmatrix} \quad (3)$$

5.3. In-Situ measurements

The antenna orientation, i.e. the alignment of the antenna horizontal probe against true earth horizontal, was determined with a precision of $\pm 1^\circ$ in order to avoid mixing

of the 2nd and the 3rd Stokes parameters. Correction to the measured data can be applied through (4).

$$\overline{T}_B' = \begin{pmatrix} I' \\ Q' \\ U' \\ V' \end{pmatrix} = \begin{pmatrix} 1 & 0 & 0 & 0 \\ 0 & \cos(2\theta) & -\sin(2\theta) & 0 \\ 0 & \sin(2\theta) & \cos(2\theta) & 0 \\ 0 & 0 & 0 & 1 \end{pmatrix} \begin{pmatrix} I \\ Q \\ U \\ V \end{pmatrix} \quad (4)$$

Finally the target surface temperature has been monitored continuously using a thermal infrared camera and a hand-held thermometer.

6. MEASUREMENT RESULTS

Target configurations with layer thickness from 2 cm to 32 cm have been measured for the wood/styrodur setup. Typically the target was clockwise rotated 15° for each data point in order to limit the total experiment duration. Results from the experiment (layer thickness 2 cm and 8 cm) are presented in Figure 6, where the solid lines are simulated responses, based on [6]. All curves have been adjusted to zero mean in order to fit into the same scale.

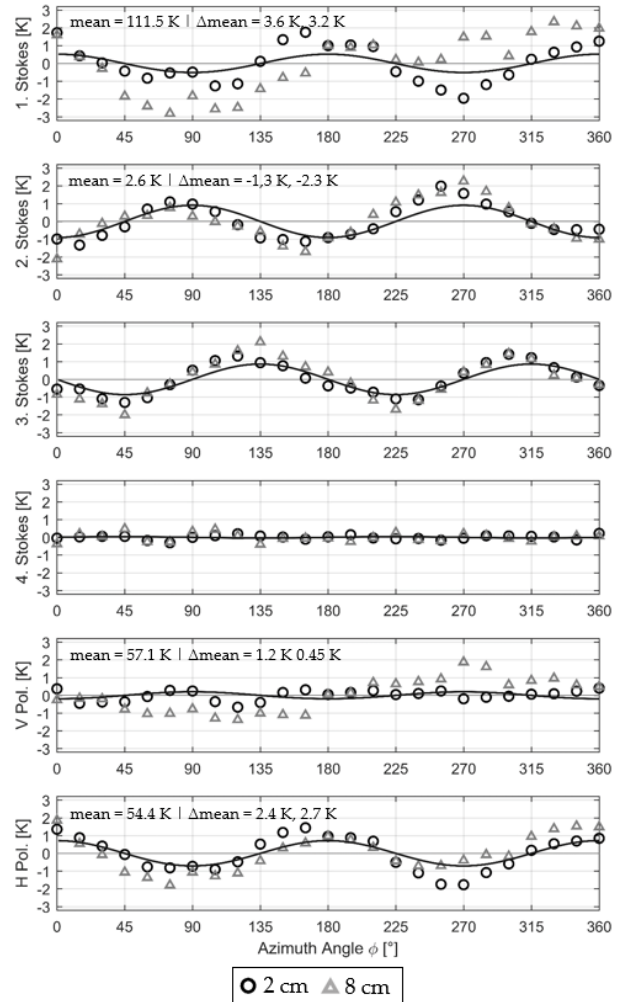


Figure 6: 360° - Polarimetric measurements for alternating wood/styrodur rows with a thickness of 2 cm and 8 cm each.

The measured results for a layer thickness of 2 cm indicate a very clear sinusoidal signature in the 1st, 2nd, and 3rd Stokes parameter, as well as in the horizontal polarization. According to [6], the magnitude of the sinusoidal signature is determined by the permittivity difference, $\Delta\epsilon'$, which is ≈ 2.5 for wood and styrodur. Simulated magnitudes are found to be 1.5 K - 2 K, and measured responses are in good agreement with the simulations. For V-polarization, the simulated response is ≈ 0.5 K, but for this channel, the correlation between measured and simulated response is less pronounced. Finally, the 4th Stokes parameter shows a very small response, ≈ 0.1 K, for both simulation and experiment, where system effects might become influential/dominant.

Very similar results are found from the experiments with layer thickness 4 cm (not shown) and 8 cm. For layers of 16 cm, magnitudes significantly drop, except for H-pol, and hence for the 2nd Stokes parameter. Finally, for 32 cm layers, all responses are reduced to less than half the expected magnitudes, and responses are no longer identified as clearly sinusoidal. From these results, it is concluded that the model seems to break down around $\lambda/2$, which is in agreement with the model theory in [6].

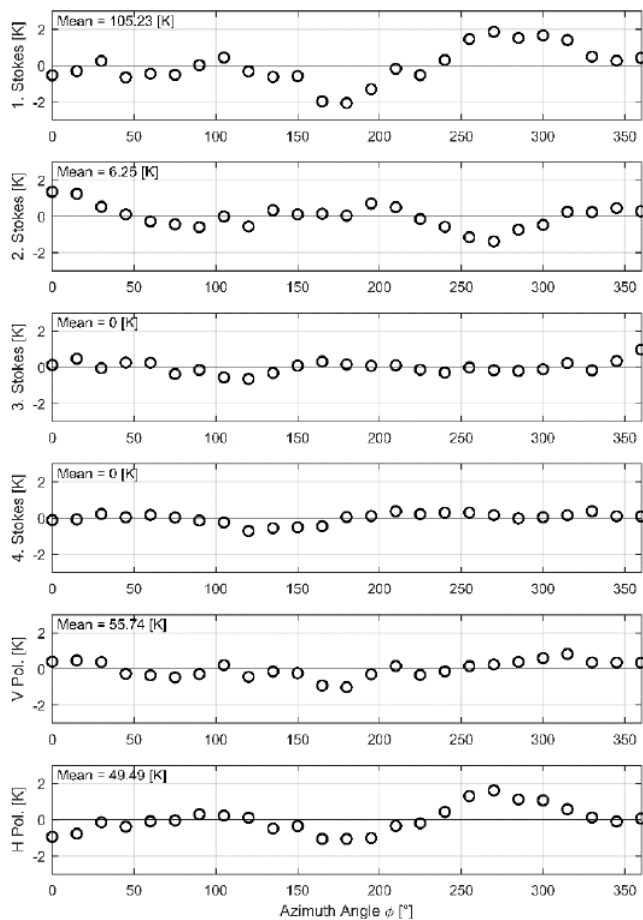


Figure 7: 360° - Polarimetric measurement results for soil/open water in 40 cm row spacing.

Changing the target for soil/open water in rows of 40 cm as illustrated in Figure 4, the model expects magnitudes up to more than 10 K, while measured results show very small values as seen in Figure 7. Again the model seems invalid due to the high layer thickness.

7. FIRST CONCLUSIONS

This paper shows the first measurement results from a controlled field experiment, aiming at quantization of expected magnitudes of azimuthal Stokes parameter signatures at L-band, induced by permittivity differences within azimuthally aligned layers forming a smooth surface.

Expected signatures are computed from the emission model presented in [6], and for thin layers ($< \lambda/2$), a very good agreement is found between model computations and measured data. For thicker layers, above $\lambda/2$, measured data clearly shows a decreasing magnitude, and responses are no longer identified as clearly sinusoidal. In conclusion, the model seems to break down around $\lambda/2$, and significantly overestimate the response, which experimentally confirms theoretical indications in [6].

8. REFERENCES

- [1] Kraus, J. D., *Radio Astronomy*, McGraw-Hill, New York 1966
- [2] Entekhabi, D., et al., "The Soil Moisture Active Passive (SMAP) Mission", *Proc. of the IEEE*, 98, 704-716, 2010.
- [3] Macelloni, G., et al., "Effects of spatial inhomogeneities and microwave emission enhancement in random media: An experimental study", *IEEE Trans. on Geoscience and Remote Sensing*, 34(5), 1084-1089, 1996.
- [4] Søbjerg, S.S and Skou, N. "Polarimetric Signatures from a Crop Covered Land Surface Measured by an L-band Polarimetric Radiometer", *IEEE Proc. of IGARSS 2003*, July 2003.
- [5] Tsang, L., "Polarimetric Passive Microwave Remote Sensing of Random Discrete Scatterers and Rough Surfaces", *Journal of Electromagnetic Waves and Applications*, 5(1), 41-57, 1991.
- [6] Soellner, M., "Vollpolarimetrische Helligkeitstemperatur-Verteilungen von natürlichen und künstlichen Objekten bei einer Frequenz von 90 GHz", PhD Thesis, Technical University of Munich, Munich, Germany (in German), 1997.
- [7] Montzka, C., et al., "Brightness temperature and soil moisture validation at different scales during the SMOS Validation Campaign in the Rur and Erft catchments, Germany" *IEEE Trans. on Geoscience and Remote Sensing*, 51(3): 1728-1743.
- [8] Born, M. and Wolf, E. "Principles of optics: Electromagnetic theory of propagation, interference and diffraction of light". *CUP Archive*, 2000.
- [9] Jonard F., et al., "Estimation of hydraulic properties of a sandy soil using ground-based active and passive microwave remote sensing", *IEEE Trans. on Geoscience and Remote Sensing*, 53(6): 3095-3109, 2015.
- [10] Søbjerg, S.S., et al. "The Airborne EMIRAD L-Band Radiometer System", *IEEE Proceedings of IGARSS 2013*, 2013.